Deep Learning-Based for Automatic Multi-Landmark Localization in Medical Images

Alexandre Pauly, National Yang Ming Chiao Tung University student

***Abstract*— With the unprecedented developments in deep learning, automatic landmarks detection of main abdominal organs seems to be a solved problem as state-of-the-art (SOTA) methods have achieved comparable results with inter-rater variability on many benchmark datasets. But, in this study, we propose a simplistic and effective technique for detecting landmarks in medical images with a U-Net convolutional neural network (CNN) architecture. Our approach using the U-Net's powerful capabilities to detect landmarks. We leverage a hierarchical U-Net model to integrate global and local localization strategies. Initially, the global U-Net segments anatomical structures in the entire image, providing a rough localization of landmarks. Subsequently, local refinement is performed using smaller regions around the globally identified landmarks. This refinement is achieved through iterative processing with specialized U-Net modules, focusing on the precise localization of landmarks within localized regions. The evaluation was carried out by locating 19 landmarks in the cephalometric images. These 19 landmarks are used to ensure a detailed and accurate assessment of the craniofacial structures, which is crucial for effective diagnosis and treatment plans in orthodontics and maxillofacial surgery.**

***Index Terms*— Landmark localization, convolutional neural network, deep learning, cephalometric X-ray.**

I. Introduction

IDENTIFICATION of anatomical landmarks is essential for numerous medical image analysis tasks, such as image registration, the initialization of segmentation methods, and the calculation of clinical measurements for patient diagnosis and treatment planning. Although manual identification of anatomical landmarks is often straightforward, it can be labor-intensive and time-consuming. Automatic landmark localization methods, which are fast and precise, can replace this manual identification, especially when multiple landmarks need to be accurately located.

Many application-specific methods have been proposed for automatic landmark localization. These methods often combine the segmentation of structures containing the landmarks with analysis based on local rules. More general approaches use multi-atlas image registration or machine learning. In multi-atlas image registration, several atlas images with annotated landmarks are aligned to the target image, and then a voting system determines the landmarks' locations. While these approaches are accurate and resilient to the limited diversity of anatomy and image acquisition, they are generally very slow.

Machine learning offers a faster and more robust alternative. Traditional machine learning approaches for landmark localization in medical images often rely on classification or regression. These methods frequently depend on a carefully chosen final threshold, specific to the data and task. Regression-based methods avoid the use of a strict threshold by producing continuous values, thus predicting the displacement or distance relative to the landmark from image slices or voxels.

In this context, we focus on the use of deep neural networks for landmark detection. The goal is to combine simplicity and efficiency in landmark localization.

For this, the rest of the paper is organized as follows. In first, we highlights related works on the same subject. After that, we present and analyse Cephalometric X-rays dataset. Afterwards, we conduct a comprehensive study for landmarks detection with the method U-Net. Next we will analyse the results and finally, in the last section, the conclusions are drawn.

II. Related works

Like many other automatic image analysis tasks, automatic landmark localization methods are now primarily based on deep learning. Deep learning methods outperform conventional machine learning methods across a wide range of applications. The advantage of deep learning is that it does not require manual feature engineering. Several deep learning methods have been proposed for landmark localization using classification. For example, Yang et al. [3] classified image slices using a convolutional neural network (CNN) and predicted the location of a landmark by intersecting the classification results of all axial, coronal, and sagittal slices. Zheng et al. [1] localized a landmark by classifying image voxels using multi-layer perceptrons, while Arik et al. [4] performed pixel classification using a CNN to locate landmarks. Xu et al. [5] localized landmarks using a CNN that classified pixels based on their relative position (above, below, left, or right) concerning the landmark.

These methods identified landmarks using pixel-wise action steps. Deep learning-based methods that leverage regression often predict heatmaps representing the distance between evaluated voxels and the landmark of interest. Landmarks are identified as local or global minima in these heatmaps. The voxel labels in the heatmaps can be viewed as pseudo-probabilities, indicating the proximity of a voxel to a landmark. This makes heatmap regression comparable to voxel classification without using a strict threshold. Wolterink et

al. [6] used a CNN with dilated convolutions to predict heatmaps indicating landmark locations. Similarly, Payer et al. and O'Neil et al. proposed heatmap prediction methods for automatic landmark localization. Payer et al. [7] used a CNN that combined local appearance responses of a single landmark with the spatial configuration of that landmark relative to all other landmarks, while O'Neil et al. [2] used a CNN that analyzed low-resolution images and then used a second CNN for further refinement. Torosdagli et al. [17] used a CNN to predict heatmaps representing the geodesic distance to a segmented organ containing landmarks and then used a long-term memory classification network to localize closely placed landmarks.

Contrary to methods performing a single task at a time, Meyer et al. [9] used a multitask network to determine the closest landmark to an analyzed pixel and then predicted the normalized 2D distance to that landmark. Heatmap regression often requires combining a large number of predictions, such as through a majority voting strategy, making it computationally expensive and time-consuming. Therefore, Zhang et al. [8] chose a different approach, using a CNN to predict displacement vectors indicating the distance and direction of an analyzed voxel to the landmark of interest.

Subsequently, the CNN architecture was complemented by additional layers to model the correlations between analyzed input patches and predicted landmark coordinates. Despite achieving good results, predicting landmark coordinates directly from the image can be prohibitive for complex, large-scale CNN architectures modeling non-linear correspondences between the input image and the landmark location. Besides deep learning-based regression methods that directly predict landmark locations, regression has also been used to iteratively determine landmark locations in an image. Aubert et al. [11] used a network to regress the displacement from an initial input patch, chosen using a statistical shape model, to the reference landmark. The landmark position was obtained by iteratively moving the input patch, using the predicted displacements, until convergence and landmark localization. Li et al. [12] iteratively localized landmarks using a CNN that predicted the distance along each of the three coordinate axes from the center of 2.5D patches to the landmark of interest while using classification to predict positive or negative movement along each coordinate axis. Ghesu et al. [13], Alansary et al. [14], and Al et al. [15] localized landmarks by exploiting deep reinforcement learning to find the optimal search trajectory from an initial starting point to the point of interest.

Julia M. H. Noothout et al. [19] proposed a global-to-local localization approach, where an initial FCNN predicts the global locations of multiple landmarks simultaneously, followed by specialized FCNNs for final refinement of each landmark's location. The global localization of multiple landmarks and subsequent local localization of a single landmark are performed similarly. While previous landmark localization methods used either classification or regression approaches, they proposed a fully convolutional neural network based on patches that performs both classification and regression. A patch-based approach is computationally efficient compared to voxel-based approaches. However, since patch-based classification is inherently less precise than its voxel-based counterpart, this issue is mitigated by jointly regressing displacement vectors pointing to the landmark's location. Conversely, using a regression-only localization approach could lead to suboptimal localization results. Combining regression and classification results in a landmark localization method that is both fast and highly accurate. They demonstrated that their method is generally applicable to various landmark localization tasks: 8 landmarks in 3D coronary computed tomography angiography (CCTA) scans, 2 landmarks in 3D olfactory MRI scans, and 19 landmarks in 2D cephalometric X-rays. Moreover, they showed that they could localize single and multiple landmarks simultaneously. In this study, we will compare our results with theirs on multiple segmentation tasks.

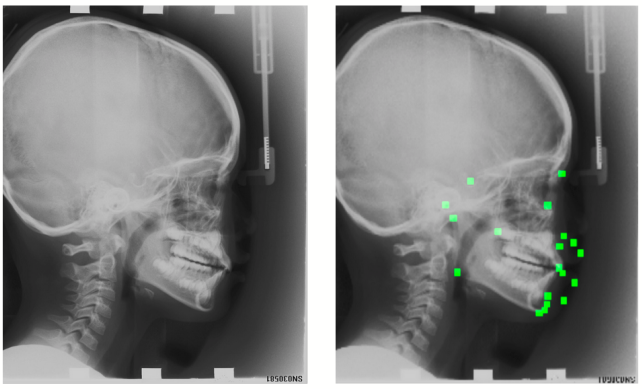

Fig. 1. Overview of the Cephalometric X-Rays dataset.

III. Cephalometric X-Rays dataset

The dataset (**Fig. 1**) contain 400 publicly available cephalometric X-rays (lateral cephalograms) from the ISBI 2015 Grand Challenge in Automatic Detection and Analysis for Diagnosis in Cephalometric X-ray Images. The X-rays were obtained using a Soredex CRANEX® Excel Ceph machine (Tuusula, Finland) and Soredex SorCom software, and were provided in TIFF format with a resolution of 1935 × 2400 pixels. In each X-ray, two experienced medical doctors manually annotated 19 clinically relevant landmarks, which are essential for diagnosis and treatment planning in orthodontic patients. According to the challenge protocol, the average of the annotations from both experts was used as the ground truth landmark locations. The landmarks included: sella (L1), nasion (L2), orbitale (L3), porion (L4), subspinale (L5), supramentale (L6), pogonion (L7), menton (L8), gnathion (L9), gonion (L10), lower incisal incision (L11), upper incisal incision (L12), upper lip (L13), lower lip (L14), subnasale (L15), soft tissue pogonion (L16), posterior nasal spine (L17), anterior nasal spine (L18), and articulate (L19) (**Fig 2**). The dataset consists of images without landmarks and CSV files containing the coordinates of the 19 landmarks for each image.

IV. Data pre-processing

After extracting and visualizing the dataset, it was observed that the input images were in JPG format and the labels were

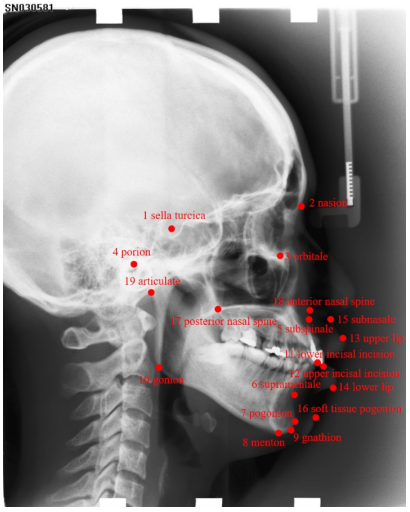

Fig. 2. Overview of a Cephalometric X-Rays labelled. Image from 'Automatic Cephalometric Landmark Detection on X-Ray Images Using a Deep-Learning Method' [18] to show the different kind of landmarks.

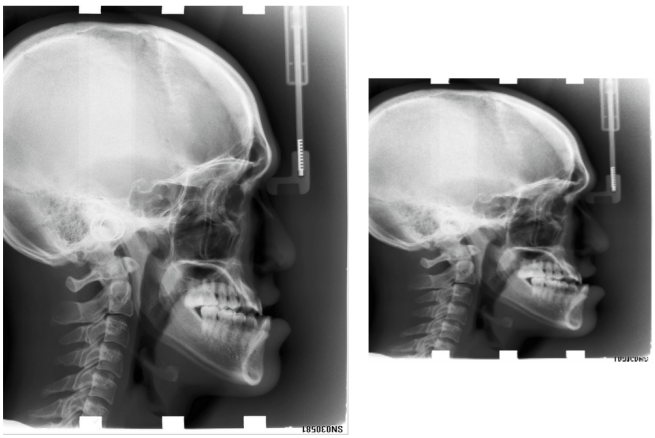

Fig. 3. Overview of the Cephalometric X-Rays resized. Original image : 1935 × 2400 pixels and resized image : 256 x 256 pixels

in a csv files as coordinates, for all data (training, validation and test). The original shape is 1935 × 2400 pixels, but to perform faster on the model, they are resized in 256 x 256 pixels.

In addition, given that the data is represented in grey levels on a scale of 0 to 255 (RGB values), it is necessary to normalise it in order to obtain values between 0 and 1. This normalisation is only applied to the model inputs. Both resizing and normalisation helps to reduce the computaniotal costs.

V. Methods used

A. Model Architecture

In this study, we developed a U-Net based architecture configured for precise landmark detection in Cephalometric X-Rays images. U-Net is a well-established convolutional neural network architecture, particularly effective for biomedical image segmentation tasks due to its ability to capture context and high-resolution localization simultaneously.

Our U-Net model follows the standard encoder-decoder structure with symmetric skip connections to retain spatial information. The input shape of the model is defined as (256, 256, 1), representing a 256 x 256 grayscale image.

The encoder path, also known as the contracting path, consists of four convolutional blocks. The first block includes two convolutional layers with 64 filters of size 3x3, each followed by Batch Normalization and ReLU activation. The output of this block is then passed through a max pooling layer with a pool size of 2x2 to reduce the spatial dimensions. This initial layer configuration captures basic edge and texture features, with Batch Normalization helping to stabilize and accelerate the training process. The second block is similar to the first but with 128 filters, allowing the model to capture more complex patterns and features as the network goes deeper. The third block further increases the number of filters to 256, enabling the detection of even more complex and abstract features. The fourth block uses 512 filters, focusing on capturing high-level features essential for accurate landmark detection.

The bottleneck, or bridge, consists of the fifth convolutional block, which includes two convolutional layers with 1024 filters, each followed by Batch Normalization and ReLU activation. This bottleneck serves as a bridge between the encoder and decoder paths, capturing the most abstract features before upsampling.

The decoder path, or expansive path, consists of four upsampling blocks. The first decoder block starts with a transposed convolution layer with 512 filters, followed by concatenation with the corresponding feature map from the encoder path. This is followed by three convolutional layers with 512 filters. Transposed convolution layers, also known as deconvolution, increase the spatial dimensions, while skip connections ensure the model retains high-resolution information from the encoder path. The second decoder block is similar to the first but with 256 filters and concatenation with the third convolutional block. The third decoder block uses 128 filters and concatenates with the second convolutional block. The fourth and final decoder block uses 64 filters and concatenates with the first convolutional block.

The output layer consists of a single convolutional layer with a 1x1 filter to produce the final segmentation map with the same spatial dimensions as the input. The sigmoid activation function is used for binary classification. The 1x1 convolutional layer reduces the feature map to the desired number of classes, in this case, one class for the landmarks, and the sigmoid activation function is appropriate for binary segmentation tasks.

B. Rationale for Design Choices

The use of 3x3 convolutional filters is a standard choice in convolutional neural networks as they are large enough to capture spatial hierarchies but small enough to retain fine details. Batch Normalization is included after each convolutional layer to stabilize and accelerate the training process by normalizing the activations. Max pooling is used in the encoder path to progressively reduce the spatial dimensions, allowing the

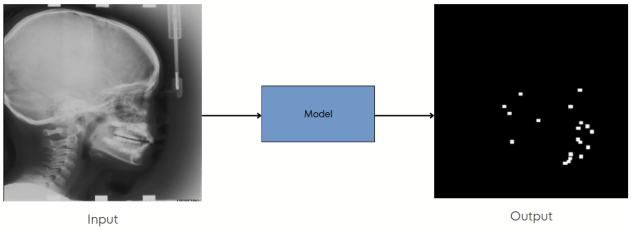

Fig. 4. Input and output of the model

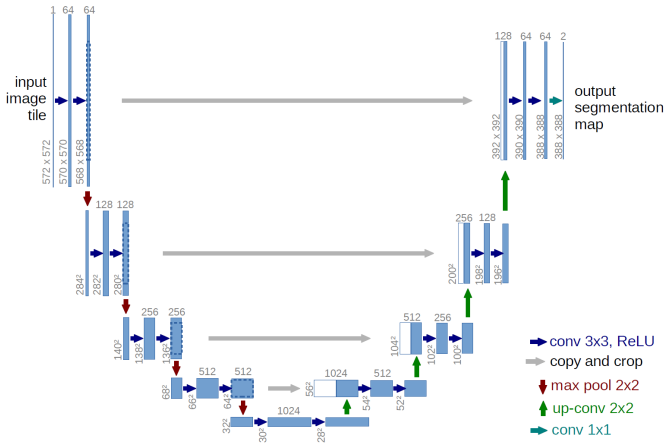

Fig. 5. Overview of U-Net architecture

network to capture hierarchical features while also reducing computational load. Transposed convolution, employed in the decoder path, progressively restores the spatial dimensions, allowing the model to make precise predictions at the pixel level. Skip connections ensure that the high-resolution features from the encoder path are directly used in the decoder path, which helps in maintaining spatial accuracy.

Overall, the carefully designed U-Net architecture allows for precise and accurate landmark detection in cephalometric images, leveraging the strengths of both convolutional layers and skip connections to handle the complexity of the task effectively.

C. Dice Coeff as Loss

For this task, we utilize the Dice coefficient as the primary evaluation metric. The Dice coefficient is particularly well-suited for measuring the overlap between two samples. It is defined as:

$$\text{Dice Coefficient} = \frac{2 \cdot |A \cap B|}{|A| + |B|}$$

where A is the set of predicted pixels and B is the set of ground truth pixels. The Dice coefficient ranges from 0 to 1, where 1 indicates perfect and complete overlap between the predicted and ground truth segmentation.

The choice of the Dice coefficient is motivated by several factors:

- Suitability for imbalanced data: In medical imaging tasks, such as cephalometric landmark detection, the regions of interest (landmarks) often occupy a small portion of the image. The Dice coefficient is less sensitive to class imbalance compared to other metrics like accuracy, making it a more reliable measure for evaluating segmentation quality.
- Focus on overlap: The Dice coefficient directly measures the overlap between the predicted segmentation and the ground truth. This is critical for our task, where precise localization and segmentation of landmarks are essential.
- Interpretability: The Dice coefficient is intuitive and easily interpretable. A higher Dice score directly correlates with better performance, making it straightforward to assess model improvements.

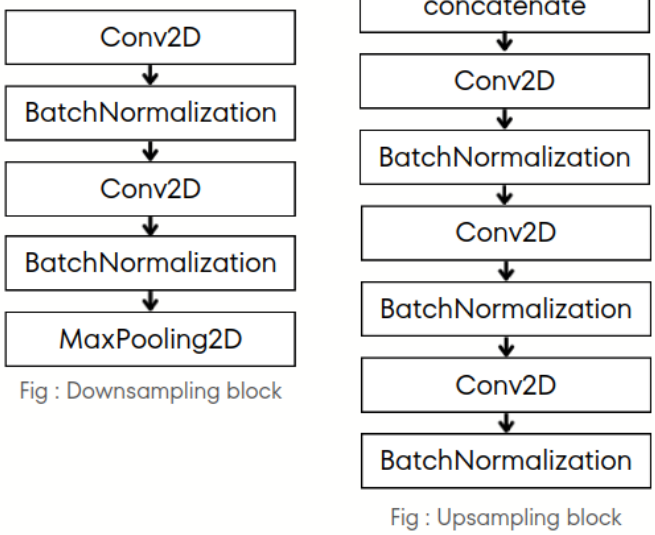

Fig. 6. Overview of U-Net architecture

D. Adam as Optimizer

For the optimization of our U-Net model, we employ the Adam optimizer. Adam, which stands for Adaptive Moment Estimation, is a widely used optimization algorithm in deep learning. It combines the advantages of two other extensions of stochastic gradient descent: AdaGrad and RMSProp. Adam computes adaptive learning rates for each parameter based on the first and second moments of the gradients. The primary reasons for choosing Adam are:

- Adaptive learning rates: Adam adjusts the learning rate for each parameter individually. This is particularly beneficial in our case as it allows the model to converge faster and more efficiently by adapting the learning rates during training.
- Robustness: Adam is known for its robustness to different types of data and hyperparameter settings. It performs well in various scenarios, including those with sparse gradients, noisy data, and non-stationary objectives. This robustness makes it a reliable choice for our model.

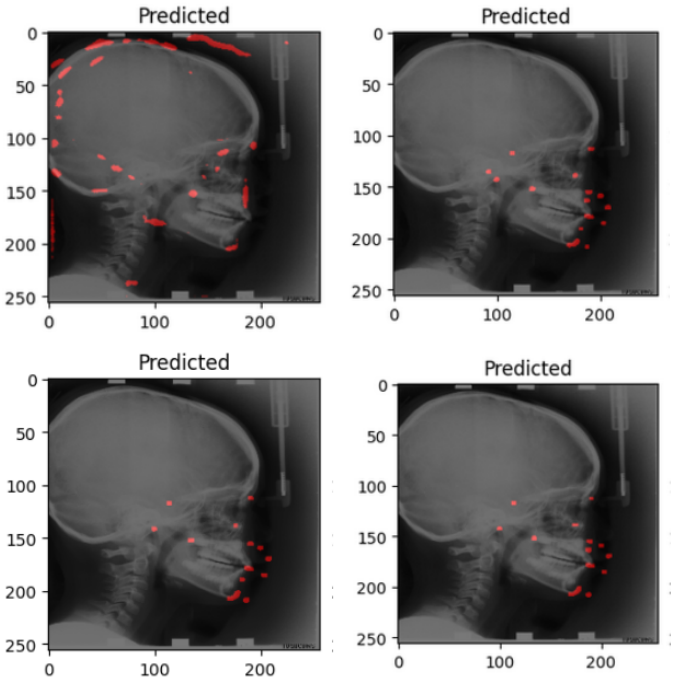

Fig. 7. Overview of predictions with different number of epochs: 20, 75, 100, and 150

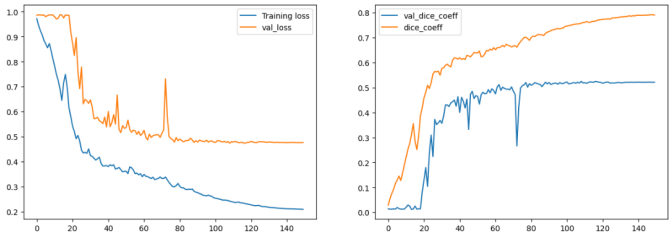

Fig. 8. Dice loss and dice coefficient with 150 epochs

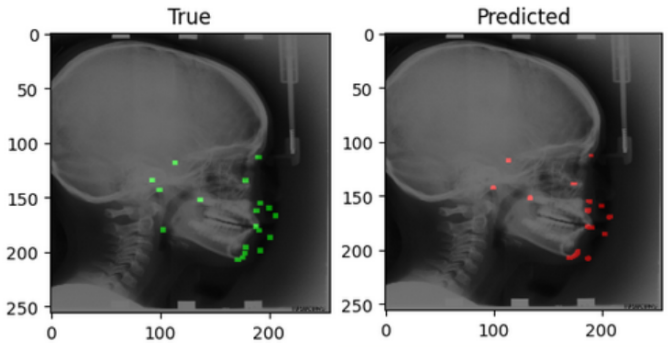

Fig. 9. Comparison between true and predicted landmarks

- Efficiency: Adam requires less memory and is computationally efficient, making it suitable for training deep neural networks. Given the complexity of our U-Net architecture, the efficiency of Adam helps in managing the training process effectively.
- Convergence speed: Adam often converges faster compared to other optimization algorithms like standard stochastic gradient descent. This accelerated convergence is advantageous for iterative experimentation and model refinement.

Now that our dataset and method have been presented, we can analyse the results in detail by comparing them with SOTA.

VI. Analysis of Results

As mentioned in the previous section, we used a U-Net model and conducted several data split tests to determine the best split. Finally, we settled on 300 images for training, 50 images for validation, and 50 images for testing.

The model was initially tested for 100 epochs. However, upon observing the loss curve, it became apparent that the model stagnated or had difficulty learning at certain periods. For this reason, we tested several significant numbers of epochs: 20, 75, 100, and 150. As shown in **Fig. 7**, there is a clear difference in results between 20 epochs and the others. Beyond 70 epochs, the model tends to stabilize, although the precision of the landmarks continues to improve slightly, and it predicts points where it was much less precise with only 20 epochs.

Interestingly, the model trained for 20 epochs contains a landmark in the neck (landmark 10 : gonion), which disappears in models trained for longer. This can be attributed to overfitting. As illustrated by **Fig. 8**, the loss function on the validation set remains stable during the first 20 epochs before dropping sharply, suggesting probable overfitting. This issue is exacerbated by the limited number of images in the dataset (400 in total). To address this, data augmentation methods, such as the use of GANs or slight image rotations, could be considered. Although this would increase the training time, the results stabilize beyond 70 epochs, with the landmarks reaching their near-final positions, except for the neck landmark.

Table 1 presents the results obtained compared to previous works. Although this comparison is based on the error range and not the median error, it still demonstrates that our model is relatively precise in locating the landmarks, as also shown in **Fig. 9**. The median distance of prediction errors for our model is 1.18 mm, which is competitive compared to existing methods.

TABLE I
COMPARISON OF RESULTS FROM DIFFERENT METHODS

Method	Error range
Julia M. H. Noothout et al.	0.46 to 2.12 mm
Lindner and Cootes	0.89 to 0.9 mm
Proposed method	0.97 to 1.32 mm

In summary, our U-Net model has proven effective for landmark detection, with stable performance beyond 70 epochs. Although the overfitting issue is notable, data augmentation techniques could further improve the results. Comparison with existing methods shows that our model is competitive, with a median error of 1.18 mm, confirming its accuracy in landmark localization. We will now discuss how to improve these results.

VII. Possible Improvements

As in the previous section on analyses, the results did not turn out as promising as expected. To enhance the model's

performance, several avenues warrant exploration:

- Try different data generation methods like a GAN model or rotating image. Rotations between -5 and 5 degrees or between 5 and 10 degrees could be more interesting than rotations of 90 degrees, for example.
- Expérimenter ce modèle sur différents datasets comme CCTA ou encore Olfactory MR
- In addition to Adam, other optimizers can be tested to determine which one best suits our segmentation problem. These include SGD, RMSprop, Adagrad, Adadelta, and Nadam.
- Exploration of new U-Net architectures: While U-Net is a reference in the field, adding or removing certain layers can significantly influence the model's performance. Variants such as U-Net++, Attention U-Net, and R2U-Net are worth exploring.
- Addition of regularization techniques: To prevent overfitting and improve model generalization, adding regularization techniques such as L1/L2 regularization, dropout, or batch normalization can be beneficial.

In this study, all the methods used focused solely on multi-landmark detection. However, an alternative approach could be to perform independent detection for each of the 19 landmarks. Each model would then be trained to detect only its own class using the appropriate loss functions and the predictions generated would be used individually for each class. To obtain a global detection of the image, the predictions of each model could be combined by superimposing the masks and assigning to each pixel the corresponding class with the highest probability at that location.

However, it is essential to continue exploring combinations of methods that have had a positive impact on the data. Testing different combinations of data augmentation, loss functions, optimisers, etc., will help to determine the optimal parameters for maximising model performance.

VIII. Conclusion

In this study, we implemented and evaluated a U-Net model for landmark detection in cephalometric images. After conducting extensive data split tests, we determined that the best configuration was to use 300 images for training, 50 images for validation, and 50 images for testing. Our model was initially tested across 100 epochs, but further investigation revealed that testing multiple significant epoch counts—namely 20, 75, 100, and 150—provided better insights into the model's performance and learning behavior.

The main limitation is that we only focus on the use of U-Net and not explored others neural networks, mainly due to computational and time limitations. Different configurations of U-Net were tested, but this one was retained.

However, the results demonstrated that our U-Net model achieved significant improvements in landmark detection accuracy beyond 70 epochs, although some overfitting was observed, particularly with the loss of certain landmarks like the neck landmark in the longer training runs. This was attributed to the relatively small dataset size, which could potentially be mitigated through data augmentation techniques such as GANs or image rotations.

Our model's performance, with a median error distance of 1.18 mm, is competitive with existing methods, as shown by comparisons with prior works. This confirms the model's precision in landmark localization and underscores its effectiveness in this application.

Future work will focus on employing data augmentation techniques to further enhance accuracy and robustness. Overall, our results confirm the U-Net model's capability in providing precise and reliable landmark localization.

References

[1] Y. Zheng, D. Liu, B. Georgescu, H. Nguyen, and D. Comaniciu, "3D deep learning for efcient and robust landmark detection in, volumetric data," in Proc. Int. Conf. Med. Image Comput. Comput. Assist. Intervent. Cham, Switzerland: Springer, 2015, pp. 565–572.

[2] A. Q. O'Neil et al., "Attaining human-level performance with atlas location autocontext for anatomical landmark detection in 3D CT data," in Proc. Eur. Conf. Comput. Vis. (ECCV), 2018, p. 5.

[3] D. Yang, S. Zhang, Z. Yan, C. Tan, K. Li, and D. Metaxas, "Automated anatomical landmark detection ondistal femur surface using convolutional neural network," in Proc. IEEE 12th Int. Symp. Biomed. Imag. (ISBI), Apr. 2015, pp. 17–21.

[4] S. Ö. Arik, B. Ibragimov, and L. Xing, "Fully automated quantitative cephalometry using convolutional neural networks," J. Med. Imag., vol. 4, no. 1, Jan. 2017, Art. no. 014501.

[5] Z. Xu et al., "Supervised action classier: Approaching landmark detection as image partitioning," in Proc. Int. Conf. Med. Image Comput. Comput.-Assist. Intervent. Cham, Switzerland: Springer, 2017, pp. 338–346.

[6] J. M. Wolterink, R. W. van Hamersvelt, M. A. Viergever, T. Leiner, and I. Iágum, "Coronary artery centerline extraction in cardiac CT angiography using a CNN-based orientation classier," Med. Image Anal., vol. 51, pp. 46–60, Jan. 2019.

[7] C. Payer, D. Štern, H. Bischof, and M. Urschler, "Integrating spatial conguration into heatmap regression based CNNs for landmark localization," Med. Image Anal., vol. 54, pp. 207–219, May 2019.

[8] D. Zhang, J. Wang, J. H. Noble, and B. M. Dawant, "HeadLocNet: Deep convolutional neural networks for accurate classication and multi-landmark localization of head CTs," Med. Image Anal., vol. 61, Apr. 2020, Art. no. 101659.

[9] M. I. Meyer, A. Galdran, A. M. Mendonça, and A. Campilho, "A pixel-wise distance regression approach for joint retinal optical disc and fovea detection," in Proc. Int. Conf. Med. Image Comput. Comput.-Assist. Intervent. Cham, Switzerland: Springer, 2018, pp. 39–47.

[10] J. Zhang, M. Liu, and D. Shen, "Detecting anatomical landmarks from limited medical imaging data using two-stage task-oriented deep neural networks," IEEE Trans. Image Process., vol. 26, no. 10, pp. 4753–4764, Oct. 2017.

[11] B. Aubert, C. Vazquez, T. Cresson, S. Parent, and J. De Guise, "Automatic spine and pelvis detection in frontal X-rays using deep neural networks for patch displacement learning," in Proc. IEEE 13th Int. Symp. Biomed. Imag. (ISBI), Apr. 2016, pp. 1426–1429.

[12] Y. Li et al., "Fast multiple landmark localisation using a patch-based iterative network," in Int. Conf. Med. Image Comput. Comput.-Assist. Intervent. Cham, Switzerland: Springer, 2018, pp. 563–571.

[13] F.-C. Ghesu et al., "Multi-scale deep reinforcement learning for real-time 3D-landmark detection in CT scans," IEEE Trans. Pattern Anal. Mach. Intell., vol. 41, no. 1, pp. 176–189, Jan. 2019.

[14] A. Alansary et al., "Evaluating reinforcement learning agents for anatomical landmark detection," Med. Image Anal., vol. 53, pp. 156–164, Apr. 2019.

[15] W. Abdullah Al and I. D. Yun, "Partial policy-based reinforcement learning for anatomical landmark localization in 3D medical images," IEEE Trans. Med. Imag., vol. 39, no. 4, pp. 1245–1255, Apr. 2020.

[16] J. Long, E. Shelhamer, and T. Darrell, "Fully convolutional networks for semantic segmentation," in Proc. IEEE Conf. Comput. Vis. Pattern Recognit. (CVPR), Jun. 2015, pp. 3431–3440.

[17] N. Torosdagli, D. K. Liberton, P. Verma, M. Sincan, J. S. Lee, and U. Bagci, "Deep geodesic learning for segmentation and anatomical landmarking," IEEE Trans. Med. Imag., vol. 38, no. 4, pp. 919–931, Apr. 2019.

[18] Song, Yu, et al. "Automatic Cephalometric Landmark Detection on X-Ray Images Using a Deep-Learning Method." Applied Sciences, vol. 10, no. 7, Jan. 2020, p. 2547, https://www.mdpi.com/2076-3417/10/7/2547.
[19] Noothout, Julia M. H., et al. "Deep Learning-Based Regression and Classification for Automatic Landmark Localization in Medical Images." IEEE Transactions on Medical Imaging, vol. 39, no. 12, Dec. 2020, pp. 4011–22. IEEE Xplore, https://ieeexplore.ieee.org/document/9139480

IX. Course feedback

I chose this course mainly to learn advanced imaging techniques, and it has more than met my expectations. I discovered the use of neural networks and understood in which contexts to adapt them, while also combining them with pre- and post-processing techniques. Additionally, the course's approach of presenting scientific papers was particularly enriching. It allowed me to step out of my comfort zone, especially regarding presentations in English. Although I'm not necessarily comfortable with English and presentations, this course helped me improve in these areas and better understand the challenges of presenting such a complex subject. I have gained valuable lessons from this experience that will benefit my future projects. Thank you for teaching this course, and best of luck in your future endeavors. I hope you will enjoy web development as much as the medical field and that you will be able to convey the same passion you have shared with us.